Control of an Electronically-Coupled Distributed Resource Unit Subsequent to an Islanding Event

Houshang Karimi, *Member, IEEE*, Hassan Nikkhajoei, *Member, IEEE*, and Reza Iravani, *Fellow, IEEE*

***Abstract*—This paper presents a new control strategy for islanded (autonomous) operation of an electronically coupled distributed generation (DG) unit and its local load. The DG unit utilizes a voltage-sourced converter (VSC) as the coupling medium. In a grid-connected mode, based on the conventional dq-current control strategy, the VSC controls real- and reactive-power components of the DG unit. Subsequent to an islanding detection and confirmation, the dq-current controller is disabled and the proposed controller is activated. The proposed controller utilizes 1) an internal oscillator for frequency control and 2) a voltage feedback signal to regulate the island voltage. Despite uncertainty of load parameters, the proposed controller guarantees robust stability and prespecified performance criteria (e.g., fast transient response and zero steady-state error). The performance of the proposed controller, based on time-domain simulation studies in the PSCAD/EMTDC software environment, is also presented.**

***Index Terms*—Autonomous operation, control, distributed generation (DG), distributed resource, dynamic model.**

I. Introduction

THE expected high depth of penetration of distributed-generation (DG) units in the utility distribution grid [1] has brought about concepts of "microgrid" [2] and "smart grid" [3]. Although full benefits of high depth of penetration of DG units are gained if a microgrid or a smart grid can be operated in both grid-connected and islanded (autonomous) modes [2], [4], the current utility practice and the existing standards [5], [6] do not permit such islanded operations. The main reason is the safety concerns associated with that portion of the utility grid that remains energized as a part of the island [7]. However, there are provisions to permit islanded operation of a DG unit and its dedicated load, if the island does not include any portion of the utility grid. In this context, the DG unit operates analogous to an uninterruptible power supply (UPS) for the load.

A technical challenge to enable an electronically-coupled DG unit and its local load to remain operational in both grid-connected and islanded modes is to equip the coupling voltage-sourced converter (VSC) with controllers that can accommodate both modes of operation and the transition process between the two modes. The conventional control strategy for an interface VSC, in the grid-connected mode, is based on current-controlled operation of the VSC [8]. In this approach, the grid dominantly dictates frequency and voltage at the point of common coupling (PCC) of the DG unit and the VSC controls its exchanged real and reactive power components with the grid based on the dq-current components.

An augmented dq-current control strategy for multiple DG units in an islanded microgrid, based on frequency/power and voltage/reactive-power droop characteristics of each DG unit, has been extensively reported [2], [4], [9]. This approach does not directly incorporate load dynamics in the control loop. Thus, large and/or fast load changes can result in either a poor dynamic response or even voltage/frequency instability.

This paper presents a novel control for autonomous operation of a VSC-coupled DG unit and its local load subsequent to islanding from the host grid. In the grid-connected mode, the interface VSC is controlled based on the conventional dq-current control strategy. Subsequent to an islanding event, the dq-current control is disabled and the proposed controller is activated. The proposed controller utilizes 1) an internal oscillator, similar to a UPS, to determine its output frequency and 2) magnitude of the PCC space vector voltage as a feedback signal to regulate the island voltage. The proposed control strategy: 1) is structurally simple; 2) guarantees robust stability of the islanded system; and 3) provides desired performance characteristics (e.g., fast transient response and zero steady-state error) for the islanded system despite uncertainties in the load parameters.

This paper develops a dynamic model of a DG unit and its local load, and presents a systematic approach to the design of the proposed controller. Based on time-domain simulation studies in the PSCAD/EMTDC software environment, performance of the control system under various islanding scenarios and imbalance load conditions are also investigated.

II. System Description

Fig. 1 shows a schematic diagram of an electronically coupled DG unit. The DG unit is represented by a dc voltage source, a VSC, a series filter, and a step-up transformer. R_t and L_t represent both the series filter and the step-up transformer. The local load is represented by a three-phase parallel RLC network at the PCC. A parallel RLC is conventionally adopted as the local load for evaluation of islanding detection methods when the load inductance and capacitance are tuned to the system frequency [5], [6]. Parameters of the system of Fig. 1 are summarized in Table I.

The DG unit and the load of Fig. 1 must remain in service in both grid-connected and islanded modes. In the grid-connected mode, the interface VSC is operated as a current-controlled voltage source which is the conventional control strategy for a

Manuscript received January 5, 2007. Paper no. TPWRD-00857-2006.

H. Karimi and R. Iravani are with the Center for Applied Power Electronics (CAPE), Department of Electrical and Computer Engineering, University of Toronto, Toronto, ON M5S 3G4 Canada (e-mail: houshang.karimi@utoronto.ca; iravani@ecf.utoronto.ca).

H. Nikkhajoei is with the Wisconsin Power Electronics Research Center, University of Wisconsin-Madison, Madison, WI 53706 USA (e-mail: nikkhajoei@wisc.edu).

Color versions of one or more of the figures in this paper are available online at http://ieeexplore.ieee.org.

Digital Object Identifier 10.1109/TPWRD.2007.911189

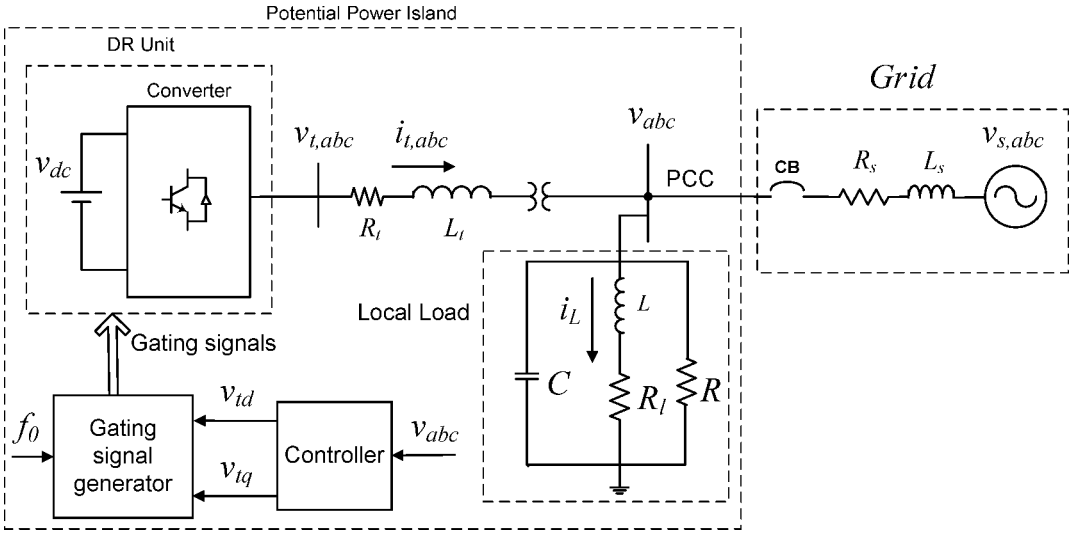

Fig. 1. Schematic diagram of a grid-interfaced DG unit and its controller.

TABLE I
PARAMETERS OF THE DG, LOCAL LOAD, AND GRID OF FIG. 1

Quantity	Value	Comment
R_t	1.5 mΩ	
L_t	300 μH	
VSC rated power	2.5 MW	
VSC terminal voltage	600 V	
PWM carrier frequency	1,980 Hz	
R	76 Ω	
L	111.9 mH	
C	62.855 μF	
Q	1.8	load quality factor
f_{res}	60 Hz	resonant frequency
R_s	1 Ω	
L_s	10 mH	
grid SCR at PCC	19.5	Short Circuit Ratio
nominal grid frequency	60 Hz	ω_0=377 rad/s
nominal grid line-line voltage	13.8 kV (rms)	
interface transformer voltage ratio	0.6/13.8 kV	Wye/Delta
interface transformer rating	2.5 MVA	
DC voltage	1500 V	V_{dcref}

VSC unit [8], [10], [11]. In the grid-connected mode, voltage magnitude and frequency of the local load, at PCC, are regulated by the grid. The VSC controls the real/reactive power exchange with the grid based on the direct-quadrature-current control method [8], [10], [11]. The scenario for which the DG unit supplies real/reactive power demand of the load and there is no real/reactive power exchange with the grid is called "matched" power condition; otherwise, it is a "mismatched" power condition.

The DG unit and the local load form an island and operate as an autonomous system by opening switch CB, Fig. 1. In an islanded mode, due to the power mismatch condition prior to the islanding instant and/or lack of control over voltage and frequency (when conventional current-controlled mode is adopted), frequency and voltage of the island drift and the island eventually becomes unstable. Therefore, to maintain uninterruptible operation subsequent to an islanding event, the event must be detected and a new control strategy that can regulate voltage magnitude and frequency of the island should be activated. The following section provides mathematical model and design of the required controls for the islanded operation. It is assumed that the islanding event is detected by a resident method in the VSC [12].

III. MATHEMATICAL MODEL OF ISLANDED SYSTEM

This section provides a state-space mathematical model for the islanded system, Fig. 1. It is assumed that the DG unit and the local load are balanced three-phase subsystems within the island. The state-space model of the islanded system of Fig. 1 in the abc-frame is

$$\begin{cases} v_{t,abc} = L_t \dfrac{di_{t,abc}}{dt} + R_t i_{t,abc} + v_{abc} \\ i_{t,abc} = \dfrac{1}{R} v_{abc} + i_{L,abc} + C \dfrac{dv_{abc}}{dt} \\ v_{abc} = L \dfrac{di_{L,abc}}{dt} + R_l i_{L,abc}. \end{cases} \tag{1}$$

In (1), $v_{t,abc}, i_{t,abc}, i_{L,abc}$, and v_{abc} are 3×1 vectors comprising the individual phase quantities (Fig. 1). Under balanced conditions, each three-phase variable x_{abc} of (1) can be transferred to a stationary $\alpha\beta$ reference frame system by applying the following abc to $\alpha\beta$ transformation:

$$x_{\alpha\beta} = x_a e^{j0} + x_b e^{j\frac{2\pi}{3}} + x_c e^{j\frac{4\pi}{3}} \tag{2}$$

where $x_{\alpha\beta} \triangleq x_\alpha + j x_\beta$. Therefore, a dynamic model of the islanded system in the $\alpha\beta$-frame is

$$\begin{cases} \dfrac{di_{t,\alpha\beta}}{dt} = -\dfrac{R_t}{L_t} i_{t,\alpha\beta} - \dfrac{v_{\alpha\beta}}{L_t} + \dfrac{v_{t,\alpha\beta}}{L_t} \\ \dfrac{dv_{\alpha\beta}}{dt} = \dfrac{1}{C} i_{t,\alpha\beta} - \dfrac{1}{RC} v_{\alpha\beta} - \dfrac{1}{C} i_{L,\alpha\beta} \\ \dfrac{di_{L,\alpha\beta}}{dt} = \dfrac{1}{L} v_{\alpha\beta} - \dfrac{R_l}{L} i_{L,\alpha\beta}. \end{cases} \tag{3}$$

We transfer (3) to a rotating reference frame based on

$$x_{\alpha\beta} = x_{dq} e^{j\theta} = (x_d + j x_q) e^{j\theta} \tag{4}$$

where $\theta(t) \triangleq \int_0^t \omega(\zeta)d\zeta + \theta_0$ is the phase-angle of an arbitrary reference vector $x_\alpha^{ref} + jx_\beta^{ref}$ in the $\alpha\beta$-frame, i.e.,

$$\theta = \arctan\left(\frac{x_\beta^{ref}}{x_\alpha^{ref}}\right). \tag{5}$$

Substituting for $\alpha\beta$ variables from (4) in (3), we deduce

$$\begin{cases} \frac{di_{t,dq}}{dt} + j\omega i_{t,dq} = -\frac{R_t}{L_t} i_{t,dq} - \frac{v_{dq}}{L_t} + \frac{v_{t,dq}}{L_t} \\ \frac{dv_{dq}}{dt} + j\omega v_{dq} = \frac{1}{C} i_{t,dq} - \frac{1}{RC} v_{dq} - \frac{1}{C} i_{L,dq} \\ \frac{di_{L,dq}}{dt} + j\omega i_{L,dq} = \frac{1}{L} v_{dq} - \frac{R_l}{L} i_{L,dq}. \end{cases} \tag{6}$$

$v_{\alpha\beta}$ is selected as a reference vector such that $v_q = 0$ and, therefore, $\dot{v}_q = 0$. The d- and q-axis components of the state variables are deduced from (6) as

$$\begin{cases} \frac{di_{td}}{dt} = -\frac{R_t}{L_t} i_{td} + \omega i_{tq} - \frac{v_d}{L_t} + \frac{v_{td}}{L_t} \\ \frac{di_{tq}}{dt} = -\omega i_{td} - \frac{R_t}{L_t} i_{tq} + \frac{v_{tq}}{L_t} \\ \frac{di_{Ld}}{dt} = -\frac{R_l}{L} i_{Ld} + \omega i_{Lq} + \frac{1}{L} v_d \\ \frac{di_{Lq}}{dt} = -\omega i_{Ld} - \frac{R_l}{L} i_{Lq} \\ \frac{dv_d}{dt} = \frac{1}{C} i_{td} - \frac{1}{C} i_{Ld} - \frac{1}{RC} v_d \\ \omega C v_d = i_{tq} - i_{Lq}. \end{cases} \tag{7}$$

In an islanded mode of operation, the VSC can employ an internal oscillator with a constant frequency $\omega_0 = 2\pi f_0$ to generate the modulating signals. Thus, the islanded system frequency ω is controlled in an open-loop manner and the VSC generates a set of three-phase voltages at frequency ω_0. Moreover, if the local load is passive, all voltage and current signals in a steady-state condition are at frequency ω_0. Therefore, assuming $\omega = \omega_0$, the last equation of (7) is a linear combination of the state variables, and leads to redundancy of one state variable. Substituting $i_{Lq} = i_{tq} - \omega_0 C v_d$ in (7) yields

$$\begin{cases} \frac{di_{td}}{dt} = -\frac{R_t}{L_t} i_{td} + \omega_0 i_{tq} - \frac{1}{L_t} v_d + \frac{1}{L_t} v_{td} \\ \frac{di_{tq}}{dt} = \omega_0 i_{td} - \frac{R_l}{L} i_{tq} - 2\omega_0 i_{Ld} + \left(\frac{R_l C\omega_0}{L} - \frac{\omega_0}{R}\right) v_d \\ \frac{di_{Ld}}{dt} = \omega_0 i_{tq} - \frac{R_l}{L} i_{Ld} + \left(\frac{1}{L} - \omega_0^2 C\right) v_d \\ \frac{dv_d}{dt} = \frac{1}{C} i_{td} - \frac{1}{C} i_{Ld} - \frac{1}{RC} v_d \\ v_{tq} = L_t \left[2\omega_0 i_{td} + \left(\frac{R_t}{L_t} - \frac{R_l}{L}\right) i_{tq} - 2\omega_0 i_{Ld} \right. \\ \qquad \left. + \left(\frac{R_l \omega_0 C}{L} - \frac{\omega_0}{R}\right) v_d\right]. \end{cases} \tag{8}$$

In (8), v_{td} and v_{tq} are the input or control signals and v_d is the only output signal which should be regulated. It should be noted that v_{tq} does not explicitly appear in (8), and is a function of state variables and parameters of the system. Since all state variables are not accessible and the load parameters are uncertain, we cannot readily calculate control signal v_{tq}. Therefore, v_{tq} is assumed to be a disturbance signal and preferably is set to zero. This assumption is reasonable since the system of (8) represents a two-degree-of-freedom (2DOF) control system. Therefore, to control the only output variable v_d, one of the two inputs suffices.

The state space equations of the potential island of Fig. 1 [i.e., (8)] in the standard state space form are

$$\begin{cases} \dot{X}(t) = AX(t) + bu(t) \\ y(t) = cX(t) \\ u(t) = v_{td} \end{cases} \tag{9}$$

where

$$\begin{aligned} A &= \begin{bmatrix} -\frac{R_t}{L_t} & \omega_0 & 0 & -\frac{1}{L_t} \\ \omega_0 & -\frac{R_l}{L} & -2\omega_0 & \frac{R_l C\omega_0}{L} - \frac{\omega_0}{R} \\ 0 & \omega_0 & -\frac{R_l}{L} & \frac{1}{L} - \omega_0^2 C \\ \frac{1}{C} & 0 & -\frac{1}{C} & -\frac{1}{RC} \end{bmatrix} \\ b^T &= \begin{bmatrix} \frac{1}{L_t} & 0 & 0 & 0 \end{bmatrix} \\ c &= [0 \quad 0 \quad 0 \quad 1] \\ X^T &= [i_{td} \quad i_{tq} \quad i_{Ld} \quad v_d]. \end{aligned} \tag{10}$$

Dynamical equations (9) describe an SISO control system in the dq-frame. To design a controller for the potential island of Fig. 1 in s-domain, a transfer function of the system is obtained from (9) as

$$g(s) = c(sI - A)^{-1} b = \frac{N(s)}{D(s)}, \tag{11}$$

where

$$\begin{aligned} N(s) &= RL^2 \left(s^2 + \frac{2R_l}{L} s + \frac{w_0^2 L^2 + R_l^2}{L^2}\right), \\ D(s) &= a_4 s^4 + a_3 s^3 + a_2 s^2 + a_1 s + a_0. \end{aligned} \tag{12}$$

a_i, $i = 0, 1, 2, 3$, are functions of the system parameters and are expressed as

$$\begin{aligned} a_4 &= L_t R L^2 C \\ a_3 &= (L_t L^2 + R_t R L^2 C + 2R_l L_t R L C) \\ a_2 &= \big(L_t R L + R L^2 + R_t L^2 + 2R_t R_l R L C \\ &\qquad + 2R_l L_t L + R_l^2 L_t R C\big) \\ a_1 &= \big(R_t R L + 2R_l R L + R_t R_l^2 R C + R_l L_t R + 2R_t R_l L \\ &\qquad + R_t \omega_0^2 R L^2 C + R_l^2 L_t + \omega_0^2 L_t L^2 - 2\omega_0^2 L_t R_l R L C\big) \\ a_0 &= R_t R_l R + \omega_0^2 R L^2 + R_t \omega_0^2 L^2 + R_l^2 R + R_t R_l^2 \\ &\qquad + \omega_0^2 L_t R L - \omega_0^2 L_t R_l^2 R C - \omega_0^4 L_t R L^2 C. \end{aligned}$$

Transfer function $g(s)$ has the following features:

- $g(s)$ has two stable zeros at $z_{1,2} = -(R_l/L) \pm j\omega_0$ and consequently is minimum phase;
- $g(s)$ represents a fourth-order system which can be unstable for specific range of load parameters R, L, and C;
- since R, L, and C are uncertain, transfer function $g(s)$ has structured uncertainty of polynomic uncertainty type [13].

Design of a robust control for this type of system is not straightforward [13] since the number of unstable poles of plant $g(s)$ are uncertain. In the following section, we design a controller for

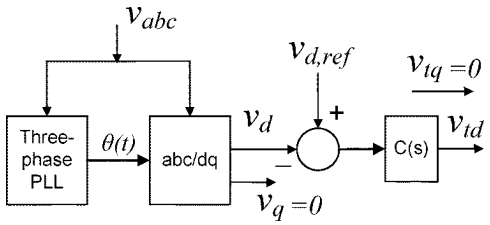

Fig. 2. Control strategy of the islanded system.

the nominal plant $g_n(s)$ and based on simulation results verify the robustness of the control system with respect to the load parameter uncertainties. The nominal plant $g_n(s)$ is obtained by substituting rated values of the load and the system parameters in (12) and (13) and is expressed as

$$g_n(s) = \frac{33150s^2 + 208300s + 4.711e9}{s^4 + 220.6s^3 + 177700s^2 + 3.094e7s + 4.868e9}.$$

IV. Control Strategy

Using the classical control approaches [14], a controller based on the transfer function of the nominal plant [i.e., $g_n(s)$] is designed. The controller should guarantee stability of the closed-loop system and provide prespecified desired performance characteristics (e.g., time response, acceptable disturbance rejection capability, and zero steady-state error to a step command input).

Fig. 2 shows a controller structure for the islanded mode. In the islanded mode of operation, load voltages v_{abc} are measured and transferred to a dq-frame. A three-phase PLL is used to provide the reference angle for the abc/dq block and thus, the q component of the load voltages is set to zero (i.e., $v_q = 0$). In such a case, the d component of the load voltages v_d should be regulated to the desired peak value of the load voltages. To regulate v_d, it is compared with reference signal $v_{d,ref}$ and the resultant error signal is applied to the designed controller $C(s)$, Fig. 2. Controller outputs v_{td} and v_{tq} are applied to the gating signal generator of the VSC (Fig. 1).

To obtain zero steady-state error $(e_{ss} = 0)$ to a step reference signal, a simple pole is assigned at the origin of s-plane. By adding another simple pole at $s = -100$ and adjusting the controller gain, the desired speed of response, overshoot, and robust stability margins are obtained. The transfer function of designed controller $C(s)$ is

$$C(s) = \frac{4000}{s(s + 100)}.$$

The designed controller is structurally simple and has a limited bandwidth which results in acceptable noise and disturbance rejection properties. Figs. 3 and 4 show the bode diagrams and the step response of the compensated closed-loop system, respectively. Fig. 3 shows that the designed controller provides gain and phase margins of 11.3 dB and 56.2°, respectively, and guarantees robust stability of the closed-loop system for the load parameter uncertainties within limits. Zero steady-state error and fast step response of the controller and the closed-loop system are observed in Fig. 4. The step response of the closed-loop system demonstrates a 44 ms rise-time.

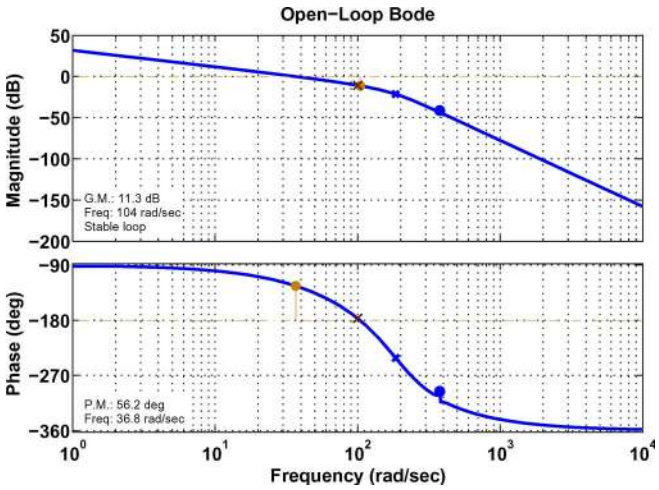

Fig. 3. Bode diagrams for the compensated system.

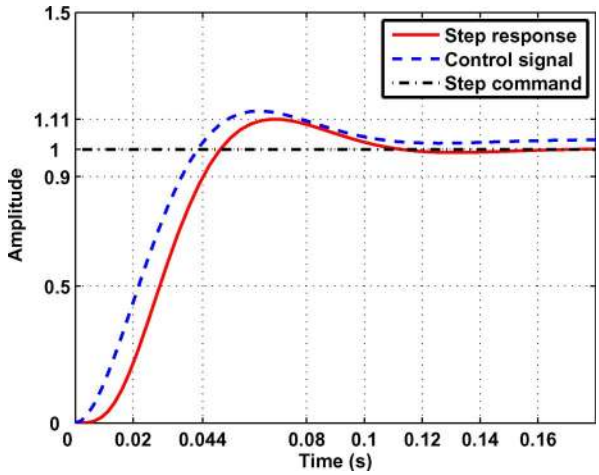

Fig. 4. Response of the controller and the closed-loop system to a step command signal.

V. Performance Evaluation

This section evaluates performance of the system of Fig. 1 during and subsequent to an islanding event, based on the proposed VSC control. The reported case studies demonstrate that the designed controller is 1) capable of maintaining the magnitude of the PCC voltage in the islanded mode and 2) robust with respect to perturbations in the load parameters. In the presented studies, it is assumed that the islanding event is detected based on an existing method and upon detection the control is changed from the conventional grid-connected control to the proposed control of Fig. 2. A signal processing approach [15] is used to estimate the sequence components of the PCC voltage. The studies are performed based on digital time-domain simulation in the PSCAD/EMTDC software environment.

A. Matched Power

The system of Fig. 1 initially operates in a grid-connected mode, where real and reactive power components of the RLC load are supplied by the DG unit. The load and the DG parameters are set at their rated values as given in Table I. The system is islanded at $\mathrm{t} = 1.0$ s by opening CB of Fig. 1, and the event

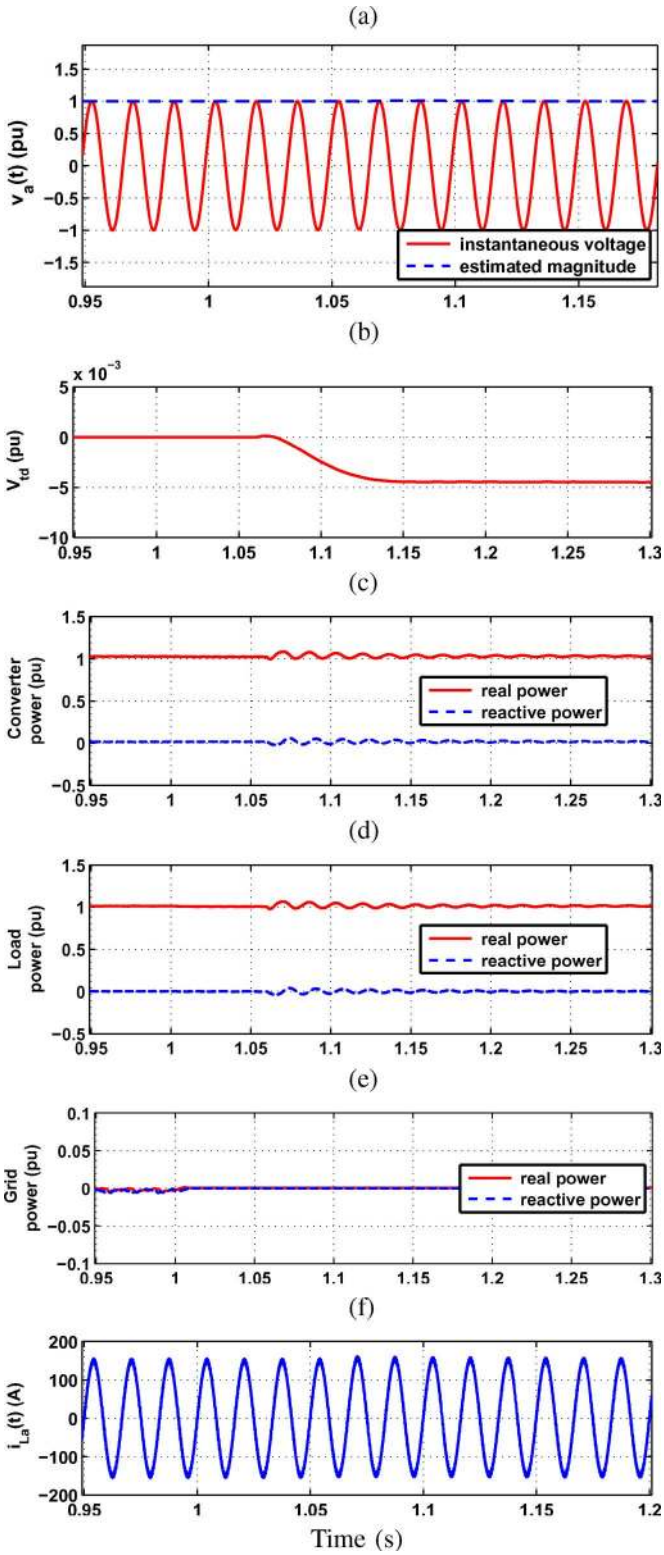

Fig. 5. Dynamic response of the system of Fig. 1 to a preplanned islanding event (a) instantaneous voltage of phase-a at PCC and its estimated magnitude, (b) control signal, (c,d,e) real and reactive power components of the converter, load, and the grid, and (f) phase-a current of the load.

is detected at $\mathrm{t} = 1.060\,\mathrm{s}$. The control strategy is changed from the grid-connected strategy (i.e., the conventional i_d/i_q control [8]) to the proposed islanded strategy of Fig. 2 at $\mathrm{t} = 1.060\,\mathrm{s}$.

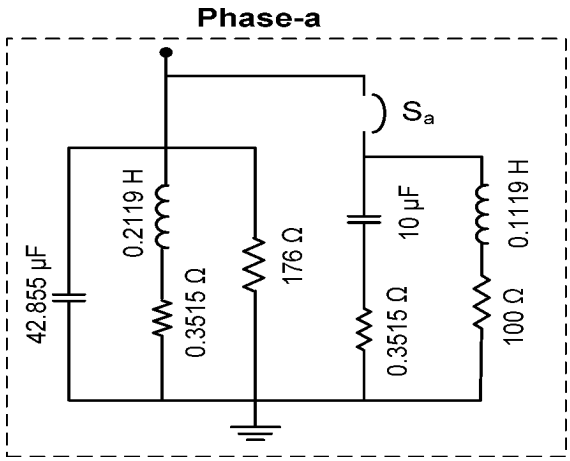

Fig. 6. Single-line diagram of the local load.

Fig. 5 shows dynamic response of the system prior, during and subsequent to the islanding event.

Fig. 5(a) shows the instantaneous voltage of phase-a at PCC and its estimated magnitude [15]. Fig. 5(a) confirms that the proposed controller maintains the load voltage after the islanding event. Fig. 5(b) shows the control signal in response to the islanding event. Fig. 5(c)–(e) shows variations of real and reactive power components of the converter, load, and the grid. Fig. 5(f) shows phase-a current of the load and demonstrates that it does not undergo a significant disturbance due to the transition from the grid-connected mode to the islanded mode and the change of controllers.

To guarantee stability and desirable performance of the islanded system, transition from the grid-connected mode to the islanded mode must be carried out smoothly. This requires that phase-angles of the internal oscillator and the dq-current controller be in a synchronous condition when the proposed controller is activated and the dq-current controller is disabled. This can be achieved by using the instantaneous control signals of the dq-current controller, at the control transfer instant, as the initial conditions for the proposed controller. Lack of smooth transition can result in long period of transients or even instability of the island.

B. Mismatched Power

The system of Fig. 1 initially operates in a grid-connected mode. The grid absorbs 1.43 MW (0.572 p.u.) real power from the converter and 710 kVAR (0.284 p.u.) reactive power from the load. The DG unit delivers real power to the system at unity power factor and the load parameters are given in Fig. 6, (S_a is open). An accidental islanding event occurs at $\mathrm{t} = 1.2\,\mathrm{s}$ and is detected at $\mathrm{t} = 1.208\,\mathrm{s}$. The islanding detection time is shorter than the previous case study since power components of the DG unit and the RLC load are not matched prior to the islanding instant and therefore the voltage magnitude at PCC and/or the islanded system frequency rapidly deviate from their acceptable limits.

Dynamic response of the system of Fig. 1 to the islanding event is shown in Fig. 7. Instantaneous voltage of phase-a and its estimated magnitude at the PCC are shown in Fig. 7(a). It is observed that after three cycles of transients, the load voltage is regulated at the desired reference value of 1.0 p.u. by the

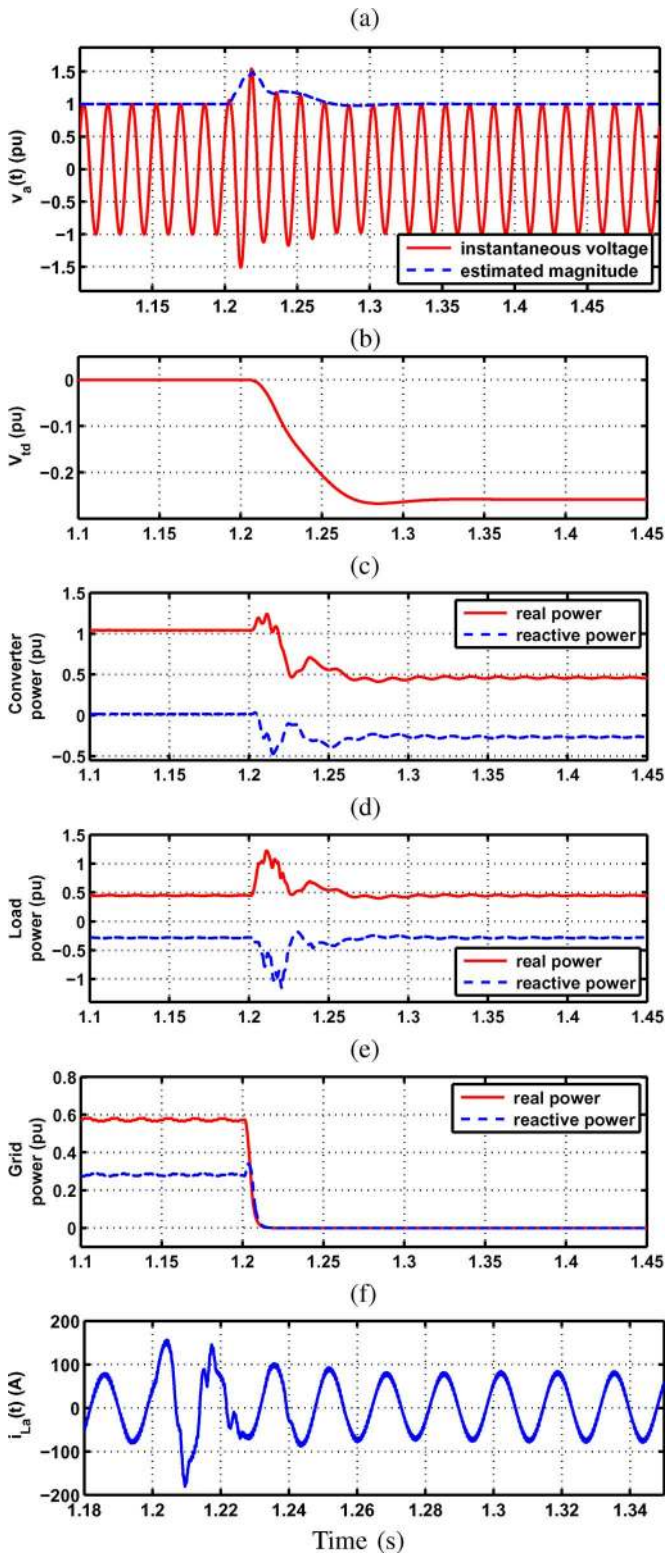

Fig. 7. Dynamic response of the system of Fig. 1 to an accidental islanding event (a) instantaneous voltage of phase-a at PCC and its estimated magnitude, (b) control signal, (c,d,e) real and reactive power components of the converter, load, and the grid, and (f) phase-a current of the load.

control system of Fig. 2. The voltage transients are as a result of power mismatch condition prior to the islanding event. Fig. 7(b) shows the control signal in response to the islanding event. Fig. 7(c)–(e) shows variations of real and reactive power components of the converter, load, and the grid, respectively. Fig. 7(f) shows load current of phase-a prior, during and subsequent to the islanding event, and demonstrates that the proposed controller can readily adjust the current to its preislanding steady-state condition within 2.5 cycles.

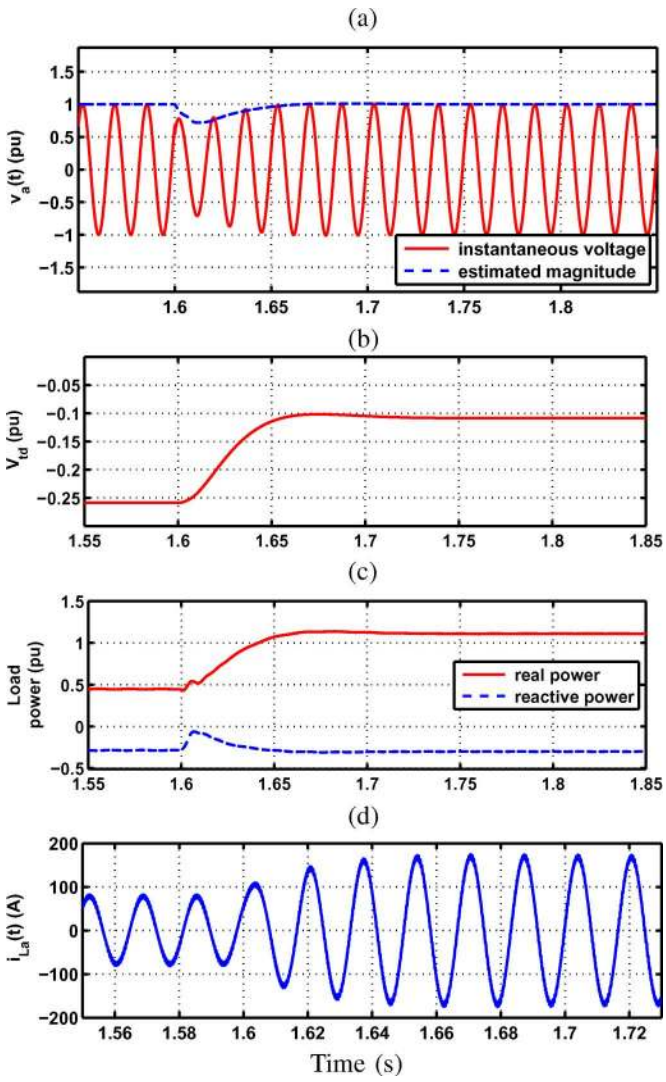

Fig. 8. Performance of the islanded system to a change in load parameters. (a) Instantaneous voltage of phase-a at PCC and its estimated magnitude. (b) Control signal. (c) Real and reactive power components of the load. (d) Phase-a current of the load.

C. Change of Load Parameters

This study case verifies robust stability and performance of the islanded mode control with respect to the load parameter uncertainties. While the system is operating in an islanded mode and under balanced conditions, the load parameters in the three phases are equally changed such that the resultant load is still balanced. The load change is imposed by closing switch S_a of Fig. 6 at $\mathrm{t} = 1.6$ s.

Fig. 8 shows the simulated system response to the load change. Fig. 8(a) shows the instantaneous voltage of phase-a and its estimated magnitude at the PCC. Fig. 8 shows that the designed controller is robust with respect to the load parameter uncertainties, and within three cycles retains magnitude of the

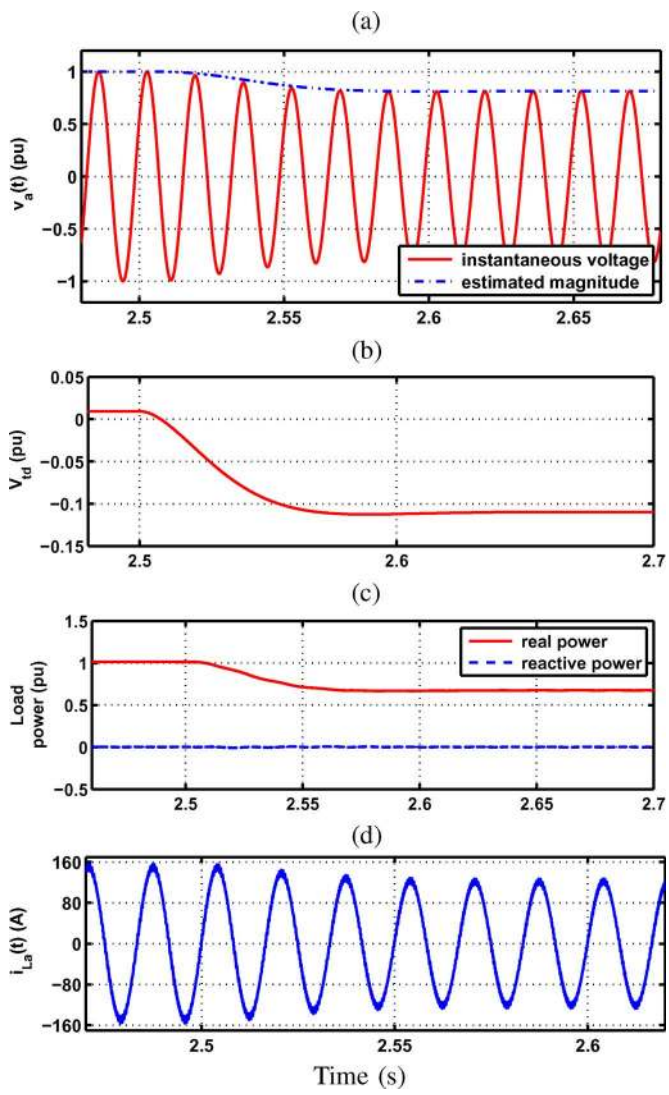

Fig. 9. Dynamic performance of the islanded system to a step voltage command. (a) Instantaneous voltage of phase-a at PCC and its estimated magnitude. (b) Control signal. (c) Real and reactive power components of the load. (d) Phase-a current of the load.

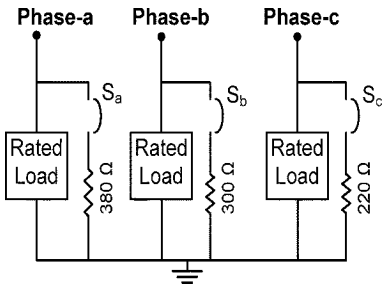

Fig. 10. Three-phase unbalanced load.

load voltage at its desired value. Fig. 8(b) shows the control signal in response to the load change. The load power components and phase-a current are shown in Fig. 8(c) and (d), respectively.

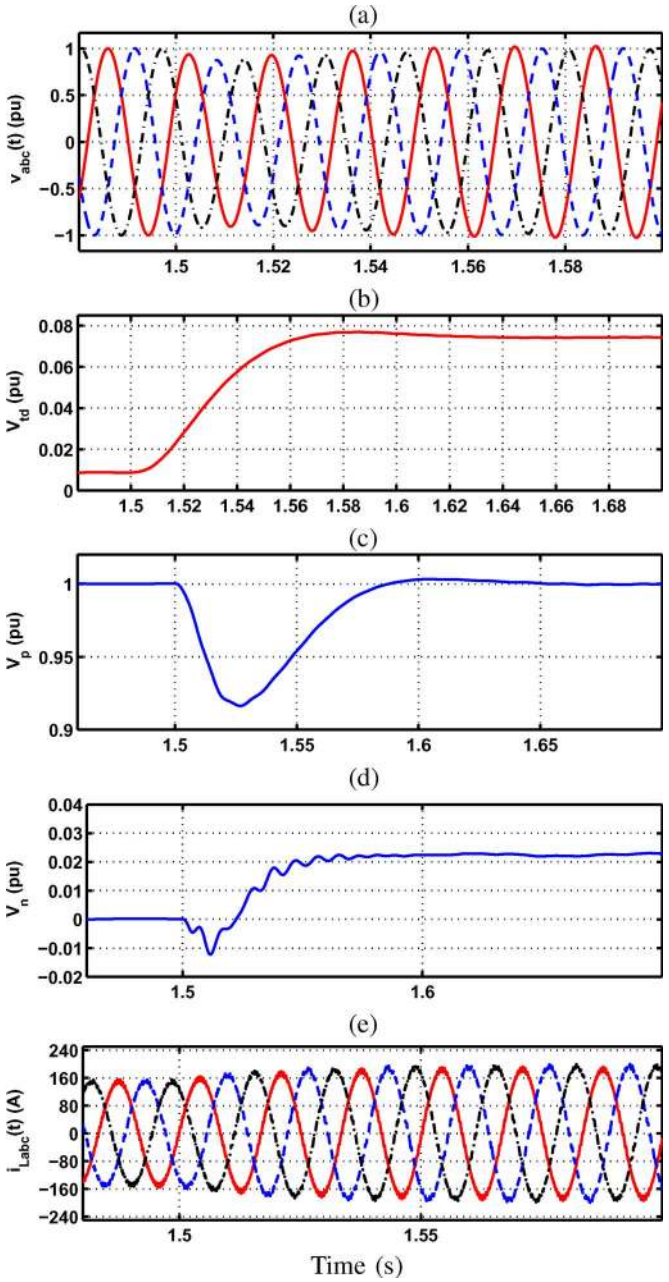

Fig. 11. Performance of the islanded system for an unbalanced condition. (a) Instantaneous load voltages. (b) Control signal. (c,d) Estimated magnitude of positive- and negative-sequence components of PCC voltages. (e) Instantaneous currents of the load.

D. Voltage Tracking

This case study demonstrates performance of the designed controller under an islanded condition in terms of reference signal tracking. While the system is operating in the islanded mode, the voltage reference signal is stepped down from 1 to 0.82 p.u. at $t = 2.5$ s. The load parameters are set at their rated values as given in Table I. Fig. 9 shows the system response to the reference change. Fig. 9(a) shows the instantaneous voltage of phase-a and its estimated magnitude at the PCC. Fig. 9(a) demonstrates that the load voltage is regulated at the new reference value of 0.82 p.u. by the designed control system within four cycles. Fig. 9(b) shows the control signal in response to the

step voltage change. Power components and phase-a current of the load are shown in Fig. 9(c) and (d), respectively. The presented time responses verify that the proposed control system of the islanded mode is capable of tracking the reference signal with zero steady-state error.

E. Load Unbalance

In this case study, while the system is initially operating in an islanded mode as a balanced system, the load parameters are changed such that the islanded system becomes unbalanced. Fig. 10 shows the unbalanced load diagram, where the rated load is the parallel RLC network used in Section V-A. Switches S_a, S_b, and S_c are initially open and simultaneously close at $\mathrm{t} = 1.5$ s and the load becomes resistively unbalanced. This switching event results in $R_b = \%95R_a$ and $R_c = \%89R_a$. Magnitudes of sequence components of the load voltage are estimated based on the method described in [15].

Dynamic response of the islanded system to the unbalanced condition is depicted in Fig. 11. Fig. 11(a) and (b) shows instantaneous load voltages and the control signal, respectively. Fig. 11(a) indicates that the designed controller maintains the load voltage at the desired reference value of 1.0 p.u. within three cycles after the switching event. Fig. 11(c) and (d) shows the estimated magnitudes of positive- and negative-sequence components of the PCC voltages. Fig. 11(d) shows that the load voltages exhibit a negative-sequence component of 2.25% which is acceptable in terms of power quality requirements [16]. The reason the load voltages become unbalanced is that the DG unit generates a set of balanced three-phase voltages and cannot compensate the unbalanced condition introduced by the load. The control signal v_{td} is also polluted by a small-amplitude, 120 Hz ripple component. The ripple component in the control signal is the result of the load voltage imbalance which appears in the dq-frame as a double-frequency 120 Hz component. The instantaneous three-phase currents of the load are depicted in Fig. 11(e). This case study verifies that the proposed controller is capable of partially compensating the unbalanced condition, however, it cannot necessarily cope with large unbalanced load conditions.

VI. Conclusion

A dynamic model and a control strategy for autonomous operation of an electronically coupled DG unit and its local load, subsequent to islanding from the utility power grid, are presented in this paper. The dynamic model is based on a state-space representation of the DG unit and the load in a dq-frame, and the classical control approach is adopted to design a robust controller for the interface converter of the DG unit. In the grid-connected mode, based on the conventional dq-current control strategy, the interface converter controls real- and reactive-power components of the DG unit. Subsequent to an islanding event, the dq-current controller is disabled and the proposed controller is activated.

The proposed controller uses an internal oscillator to control the frequency, and a voltage feedback signal to regulate the island voltage. The proposed controller guarantees robust stability and desired performance (e.g., fast transient response and zero steady-state error) despite uncertainties in the load parameters.

Performance of the proposed controller under: 1) accidental and planned islanding events; 2) uncertainties in the load parameters; 3) step changes in the control command; and 4) unbalanced load conditions are reported. The studies are carried out based on time-domain simulations in the PSCAD/EMTDC software environment. The simulation results verify effectiveness of the proposed controller in terms of maintaining voltage, frequency and stability of the islanded system during and subsequent to islanding events.

References

[1] H. B. Puttgen, P. R. MacGregor, and F. C. Lambert, "Distributed generation: Semantic hype or the dawn of a new era?," *IEEE Power Energy Mag.*, vol. 1, no. 1, pp. 22–29, Jan./Feb. 2003.

[2] P. Piagi and R. H. Lasseter, "Autonomous control of microgrids," presented at the IEEE Power Eng. Soc. General Meeting, Montreal, QC, Canada, Jun. 18–22, 2006.

[3] S. M. Amin and B. F. Wollenberg, "Toward a smart grid: Power delivery for the 21st century," *IEEE Power Energy Mag.*, vol. 3, no. 5, pp. 34–41, Sep./Oct. 2005.

[4] F. Katiraei, M. R. Iravani, and P. W. Lehn, "Micro-grid autonomous operation during and subsequent to islanding process," *IEEE Trans. Power Del.*, vol. 20, no. 1, pp. 248–257, Jan. 2005.

[5] *Standard Conformance Test Procedures for Equipment Interconnecting Distributed Resources With Electric Power Systems*, IEEE Std. 1547.1, 2005.

[6] *Inverters, Converters, and Controllers for Use in Independent Power Systems*, UL Std. 1741, 2002.

[7] J. Stevens, R. Bonn, J. Ginn, S. Gonzalez, and G. Kern, "Development and testing of an approach to anti-islanding in utility-interconnected photovoltaic systems," Sandia Nat. Labs., Albuquerque, NM, Rep. SAND2000-1939, Aug. 2000.

[8] C. Schauder and H. Mehta, "Vector analysis and control of advanced static VAR compensators," *Proc. Inst. Elect. Eng. C*, vol. 140, pp. 299–306, Jul. 1993.

[9] F. Katiraei and M. R. Iravani, "Power management strategies for a microgrid with multiple distributed generation units," *IEEE Trans. Power Syst.*, vol. 21, no. 4, pp. 1821–1831, Nov. 2006.

[10] A. Yazdani and R. Iravani, "A unified dynamic model and control for the voltage-sourced converter under unbalanced grid conditions," *IEEE Trans. Power Del.*, vol. 21, no. 3, pp. 1620–1629, Jul. 2006.

[11] H. Song and K. Nam, "Dual current control scheme for PWM converter under the unbalanced input voltage conditions," *IEEE Trans. Ind. Electron.*, vol. 46, no. 5, pp. 953–959, Oct. 1999.

[12] H. Karimi, A. Yazdani, and R. Iravani, "Negative-sequence current injection for fast islanding detection of a distributed resource unit," *IEEE Trans. Power Electron.*, vol. 23, no. 1, pp. 1698–1705, Jan. 2008.

[13] B. R. Barmish, *New Tools for Robustness of Linear Systems*. New York: Macmillan, 1994.

[14] G. F. Franklin, J. D. Powell, and A. Emami-Naeini, *Feedback Control of Dynamic Systems*. Upper Saddle River, NJ: Prentice-Hall, 2002.

[15] M. Karimi-Ghartemani and H. Karimi, "Analysis of symmetrical components in time-domain," presented at the 48th IEEE Midwest Symp. Circuits Systems, Cincinnati, OH, Aug. 7–10, 2005.

[16] J. Driesen and T. Van Craenenbroeck, "Voltage disturbances, introduction to unbalance," *Power Quality Application Guide* Copper Development Assoc., 5.1.3, May 2002.

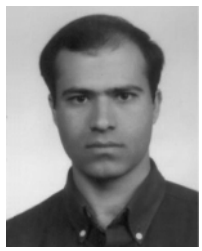

Houshang Karimi (S'03–M'07) received the B.Sc. and M.Sc. degrees in electrical engineering from Isfahan University of Technology, Isfahan, Iran, in 1994 and 2000, respectively, and the Ph.D. degree in electrical engineering from the University of Toronto, Toronto, ON, Canada, in 2007.

Currently, he is a Postdoctoral Fellow in the Department of Electrical and Computer Engineering at the University of Toronto. He was a Visiting Scientist with the Center for Applied Power Electronics (CAPE), Department of Electrical and Computer Engineering, University of Toronto, from 2001 to 2003. His research interests include distributed generation systems, power system protection, and robust control.

Hassan Nikkhajoei (M'05) received the B.Sc. and M.Sc. degrees from Isfahan University of Technology, Isfahan, Iran, in 1992 and 1995, respectively, and the Ph.D. degree from the University of Toronto, Toronto, ON, Canada, in 2004, all in electrical engineering.

Currently, he is a Research Associate in the Department of Electrical and Computer Engineering, University of Wisconsin, Madison. He was a Postdoctoral Fellow with the University of Toronto from 2004 to 2005, and a faculty member with Isfahan University of Technology from 1995 to 1997. His research interests include power electronics, distributed generation systems, and electric machinery.

Reza Iravani (M'85–SM'00–F'03) received the B.Sc. degree in electrical engineering from Tehran Polytechnique University, Tehran, Iran, in 1976 and the M.Sc. and Ph.D. degrees in electrical engineering from the University of Manitoba, Winnipeg, MB, Canada, in 1981 and 1985, respectively.

Currently, he is a Professor at the University of Toronto, Toronto, ON, Canada. His research interests include modeling and analysis of electromagnetic transient phenomena in power systems, power electronics, and power system dynamics and control.